fire

MDPI

Article

Drivers and Spatial Patterns of Burned Area in High-Andean Páramos

Jhonatan Julián Díaz-Timoté [1,*], Laura Obando-Cabrera [2], Swanni T. Alvarado [3] and Stijn Hantson [1]

[1] School of Sciences and Engineering, Universidad del Rosario, Bogotá 111221, Colombia; stijn.hantson@urosario.edu.co
[2] Yale School of the Environment, Yale University, New Haven, CT 06511, USA; laura.obandocabrera@yale.edu
[3] Departamento de Biología, Facultad de Ciencias, Universidad Nacional de Colombia—Sede Bogotá, Bogotá 110111, Colombia; stalvarador@unal.edu.co
* Correspondence: jhonatan.diaz@urosario.edu.co

Abstract

Páramos, high-mountain tropical ecosystems, are crucial for carbon storage and water regulation for many Andean cities. However, they are subjected to wildland fires that threaten the ecosystem services they provide. Fire activity varies substantially among páramos, making it essential to understand the drivers of this spatial variability. This study evaluates the relative influence of anthropogenic and biophysical factors on fire occurrence in Colombian páramos, analyzing burned area data from 2000 to 2022 using a Random Forest model. Results indicate that fire occurrence is shaped by the interaction between human pressures and biophysical characteristics. Annual precipitation was the most influential predictor: areas with lower mean annual precipitation (<1000–1500 mm/year) were linked to greater burned area. Vegetation cover, assessed using the Normalized Difference Vegetation Index (NDVI), showed a hump-shaped relationship, with intermediate greenness levels (0.13–0.25) being most prone to burning. Anthropogenic factors, especially proximity to buildings and agricultural zones, also had a significant impact. Our results show that fire occurrence in páramos cannot be attributed solely to human pressures but results from the combined effect of anthropogenic and biophysical drivers. Understanding of these interactions underscores the need for socio-ecological perspectives to guide integrated and adaptive management of strategic high-mountain ecosystems.

Keywords: paramos; fire drivers; random forest; anthropogenic pressure; tropical alpine ecosystems; Colombia; burned area

Check for updates

Academic Editor: Kevin Tansey

Received: 10 October 2025
Revised: 19 December 2025
Accepted: 8 January 2026
Published: 24 February 2026

1. Introduction

Páramos are high-mountain tropical ecosystems located primarily in the Andes. Occupying the transition zone above dense tropical mountain cloud forest until reaching glaciers, ranging from altitudes between 3000 and 4800 m [1]. Páramos cover approximately 35,000 km^2, spanning Venezuela, Colombia, Ecuador, northern Peru, and small regions in Costa Rica and Panama [2]. Páramos are highly valued for their ecosystem services, particularly as “water towers” of South America [3]. They store vast amounts of water that supply major Andean cities [4,5] and play a role as significant carbon sinks, mitigating global warming by capturing and storing atmospheric carbon [5–7]. Despite their regional importance in providing ecosystem services, páramos face growing threats from climate change, land-use expansion, and fire—one of the most frequent drivers of ecological change [5,8].

Fire of páramo has been an integral and transformative force in human-páramo interactions for thousands of years (at least 7000), and this must be acknowledged given its ecological importance [9–12]. As a result, páramos have burned relatively frequently [13], with fire acting as a natural and anthropogenic disturbance agent that influences the dynamics of vegetation [8,14,15]. Although natural phenomena such as lightning strikes and volcanic eruptions can cause fires, they alone cannot explain the historical fire patterns [11,16]. Instead, human activities have been the dominant cause to date, through deliberate land management or accidental ignition [11,16–18]. The ecological effects of páramo fires range from beneficial outcomes, such as the regeneration of fire-resistant species [19], to harmful impacts, including soil erosion, hydrological alteration, and the loss of peat and organic matter essential for carbon storage and water regulation [1,16,20]. These effects of fire and its dynamics are amplified by broader anthropogenic factors that go beyond direct burning.

On a global scale, the occurrence of fires in ecosystems has been extensively investigated and is now recognized as the emerging result of complex interactions among climatic factors, fuel availability and continuity, topography, and human activities [21,22]. These drivers operate and interact on spatial and temporal scales: climate modulates vegetation productivity and flammability, thereby defining broad windows of fire susceptibility; vegetation structure and composition determine fuel continuity; topography shapes local microclimates and influences fire spread; and human activities contribute most ignition sources and alter fuel regimes [23,24].

In contrast to other ecosystems worldwide, knowledge of fire drivers in páramo ecosystems remains scarce and fragmented, largely limited to localized case studies. Existing research highlights the influence of human access, traditional burning practices, and seasonal droughts acting on grass-dominated fuels [7,25–27]. In many páramos, fire use is closely intertwined with land-use activities such as livestock grazing and pasture renovation, the expansion of small-scale agriculture, and, in some areas, recreation and tourism [16,26]. These activities tend to concentrate ignitions near roads, settlements, and recreational facilities, creating recurrent fire fronts in accessible grasslands while leaving more remote or steep zones comparatively less affected [26]. However, only a few studies have analyzed fire occurrence patterns or quantified the relative importance of these drivers at broader spatial and temporal scales [7,13,28,29]. This limited understanding leaves key processes unexplored, particularly those explaining the spatial variability of fire occurrence, a gap that becomes increasingly concerning under climate change, which is expected to intensify fire regimes through rising temperatures and expanding human pressures [10,30].

To address this gap, our study analyzes the anthropogenic and biophysical drivers of fire in Colombian páramos. We develop a spatio-temporal analysis of burned area dynamics using the páramo Fire Atlas data [13], for the period 2000–2022, and apply a Random Forest (RF) model to identify the main drivers of the spatial pattern. We hypothesize that the spatial pattern of burned area across Colombian páramos is primarily driven by anthropogenic factors such as land use and accessibility. We further expect that biophysical conditions—including vegetation cover, climate, and altitude—modulate these patterns and contribute significantly to local variation in burned area.

2. Materials and Methods

2.1. Study Area

The study area is located in the Colombian Andes (Figure 1), which concentrates nearly half of the world's páramo ecosystems [6]. In Colombia, páramos are distributed across the three main mountain ranges and isolated massifs, forming a mosaic of landscapes shaped by strong altitudinal gradients [2]. These ecosystems are characterized by cold temperatures, frequent cloud cover, and intense solar radiation [8,16], conditions that create a distinctive microclimatic variability [31]. Such environmental heterogeneity has driven the evolution of highly specialized flora and fauna, resulting in exceptional endemism and the highest recorded plant diversity among high-mountain ecosystems worldwide [3,32]. The physiognomy evolves from a dense layer of shrubs and continuous cover of grasses, which include grasslands, frailejones (*Espeletia* sp.), puyas, acaulescent rosettes, cushion plants and herbs. At lower altitudes it is possible to find more vegetation cover, with more dense high-Andean forests and shrublands, while at higher altitudes the vegetation begins to be very sparse with shallow soils composed of rocky and sandy materials. Due to the scarcity and discontinuity of fuels, fires typically do not affect these high elevations, as noted in [31,33,34]. These transitions are accompanied by differences in soil depth, moisture, and fuel availability that are critical for understanding fire dynamics [20,25,35].

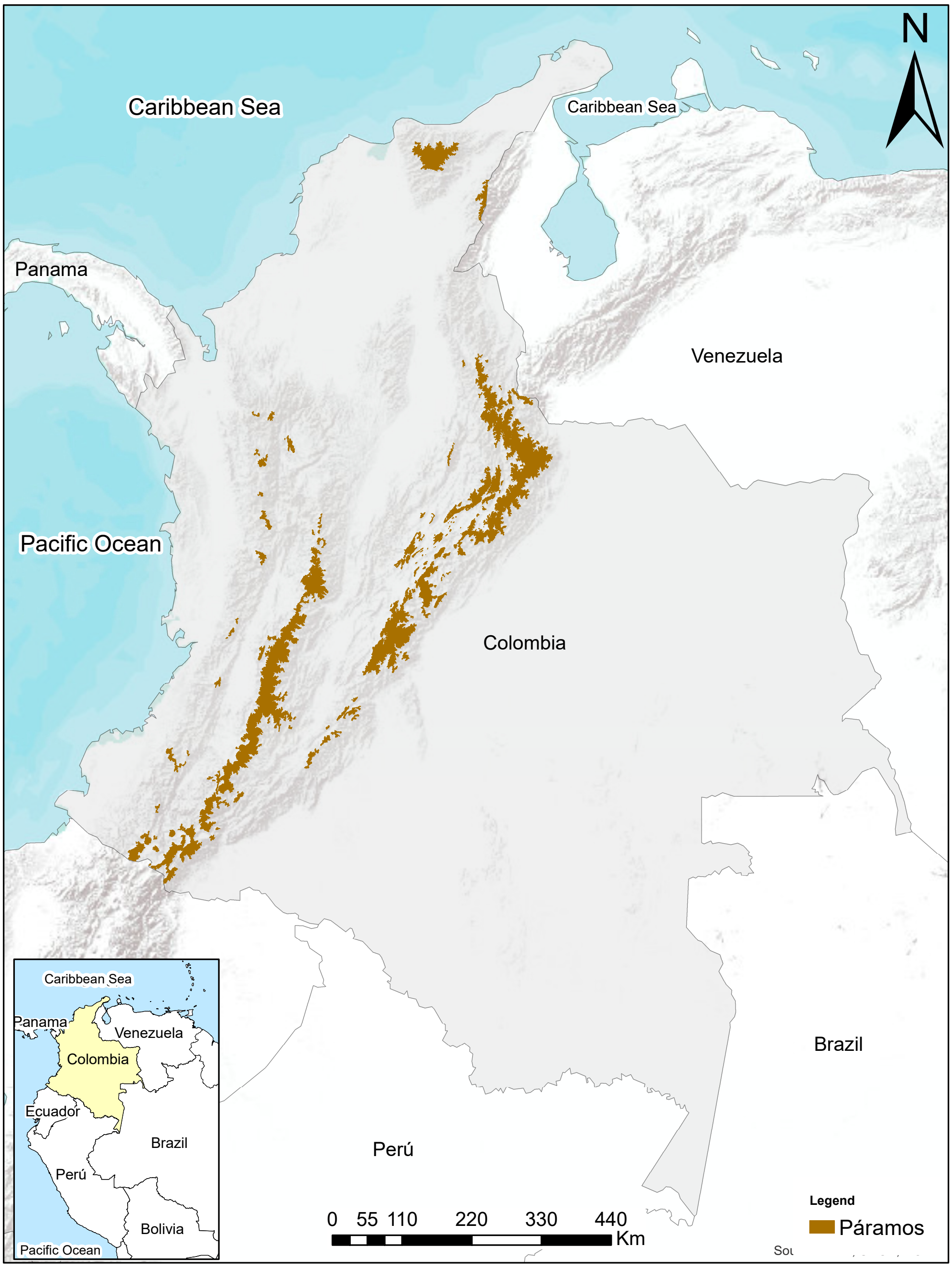

Figure 1. Location of the study area showing all Colombian páramos.

We use the same páramo area proposed in the páramo fire atlas [13] that considers the boundaries of the WWF Ecoregion map [36], a map of land cover specific to the páramos of the northern Andes [37], and the páramo map created by the Humboldt Institute [6]. This boundary also includes a 500 m buffer to account for the transition between a high-Andean forest and páramo and excludes all agricultural areas, which lets us focus on fire impact on nontransformed páramo vegetation. In this study, we use the term "páramo unit" to refer to the official complejo de páramo classification adopted by the Colombian National Environmental System (SINA) [6]. Each páramo unit represents a defined high-mountain ecosystem area with a specific name, as recognized in national environmental planning and monitoring frameworks. Similarly, each páramo unit has been geographically separated by cordillera to facilitate the spatial patterns analysis (Table A1 shows páramo units grouped by Cordillera, with burned and protected proportions).

2.2. Data Sets

2.2.1. Burned Area Data for the Páramos Unit

We examined the burned area using the Páramo Fire Atlas, a burned-area database developed for South America's páramos providing annual burned area data from 1985 to 2022 at 30 m spatial resolution [13]. The Páramo Fire Atlas applies a detection rule to ensure spatial consistency, defining the minimum mapped fire as three contiguous 30 × 30 m pixels (0.27 ha). Accuracy assessments report low commission errors (~8%) and a mean omission error of ~47%. Compared to MODIS MCD64A1, The Páramo Fire Atlas detects a higher proportion of small fires, resulting in approximately four times higher burned-area estimates. Our analysis focused on the 2000–2022 time period because pre-2000 estimates have larger uncertainty due to limited imagery availability (See Figure A1). Figure 2 shows an example of the burned area in the Tota-Bijagual-Mamapacha páramo unit in Colombia.

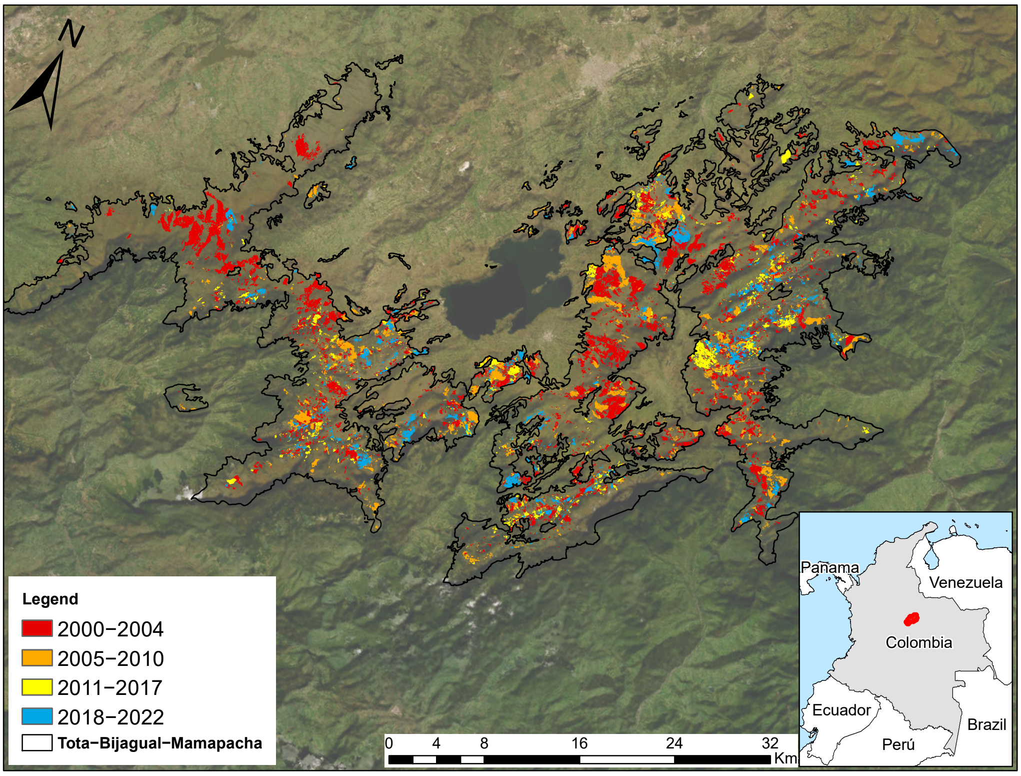

Figure 2. Example of the burned-area dataset for a representative páramo unit. The figure depicts the Tota–Bijagual–Mamapacha unit, where annual fire areas are mapped using distinct color classes.

2.2.2. Explanatory Variables

Fire dynamics in high-mountain ecosystems emerge from complex interactions among climate, vegetation structure, and human activities—processes that exhibit strong spatial heterogeneity [7]. Therefore, our variable selection was designed to represent key environmental gradients (e.g., temperature, precipitation, vegetation greenness) alongside spatial patterns of human influence (e.g., accessibility, land-use intensity, proximity to infrastructure), providing an integrated representation of the diverse factors shaping burned-area patterns.

Guided by these considerations, we compiled a comprehensive suite of eleven (11) biophysical and anthropogenic predictors hypothesized to influence burned area in páramo ecosystems; full variable descriptions, data sources, and spatial resolutions are provided in Table 1. Climatic predictors included multi-year means of maximum temperature and total precipitation, whereas human-related variables reflected socio-environmental conditions characteristic of high-Andean landscapes. Such as the human footprint and distances to buildings, forests, and roads.

Additionally, we incorporated the density of conflict events as a proxy for socio-political pressures that influence land-use dynamics in rural and high-mountain areas. "Conflict events" refer to georeferenced records of armed confrontations, attacks, and security incidents reported by official monitoring systems during the 2000–2022 period. These events are relevant because Colombia's internal armed conflict has historically shaped patterns of human access, territorial control, and land management, which can indirectly affect fire occurrence. Event density was calculated across the entire study period to derive a spatially consistent indicator. Because this variable exhibited a strongly right-skewed, near-zero distribution, it was log-transformed as $\log_{10} ConflictDens + 1 \times 10^{-6}$.

On the other hand, protected areas represent a central dimension of conservation in Colombia, where more than half of páramo regions fall under some protection category [38]. We use the database of Single registry of protected areas in Colombian páramos (RUNAP, by its Spanish acronym) [39], which are classified into four categories according to their legal restrictions: No protected areas, areas without any degree of protection, high-restriction areas, areas comprising national and regional natural parks, wildlife sanctuaries, and flora sanctuaries. Medium-restriction areas included regional and national protected forest reserves, while low-restriction areas encompassed Civil Society Nature Reserves, Regional Integrated Management Districts, and Soil Conservation Districts.

To evaluate how protection status shapes the spatial distribution of burned and unburned areas, each páramo unit was partitioned into four categories: burned inside protected areas (Burned + PA), burned outside protected areas (Burned − PA), unburned inside protected areas (Unburned + PA), and unburned outside protected areas (Unburned − PA). For each unit, these categories were normalized by the total number of pixels within their respective protection classes, allowing proportional comparisons across páramos that differ in size and in the extent of protected land. This normalization reduces bias stemming from variation in total area and protected coverage.

To evaluate whether burned area differed between protected and non-protected lands, we estimated, for each páramo unit, the proportion of burned pixels occurring inside protected areas (PAs) and the proportion occurring outside. Because these proportions were non-normally distributed and exhibited repeated values, differences between groups were tested using a Wilcoxon rank-sum test, with the exact p-value option disabled (exact = FALSE) to accommodate ties. This test provides an inferential assessment of whether protection status is associated with variation in burned area.

https://doi.org/10.3390/fire9030095

Table 1. Spatial variables used as predictors, with definitions and sources.

Spatial Variable (Abbrev.)	Description	Reference	Data Source (URL)	Resolution	Time Series
Distance to Forest (DistForest, DF)	Euclidean distance to forest was computed as the straight-line distance from each forested pixel to the nearest páramo boundary.	IDEAM (2024) [40]	https://www.ideam.gov.co/transparencia/datos-abiertos/seccion-de-datos-abiertos/resultados-monitoreo-de-bosques (accessed on 16 December 2025)	30 m	2024
Distance to buildings (DistBuildings, DB)	Euclidean distance to buildings was computed as the straight-line distance from each building to the nearest páramo boundary.	IGAC (2022) [41]	https://www.colombiaenmapas.gov.co/?e=-82.43784778320864,-0.17644239911865092,-71.23179309571162,9.90326984502256,4686&b=igac&u=0&t=23&servicio=205 (accessed on 16 December 2025)	60–100 m	2016–2022
Distance to roads (DistRoads, DR)	Euclidean distance to roads (km) was computed as the straight-line distance from each road to the nearest páramo boundary.	IGAC (2022) [41]	https://www.colombiaenmapas.gov.co/?e=-82.43784778320864,-0.17644239911865092,-71.23179309571162,9.90326984502256,4686&b=igac&u=0&t=23&servicio=205 (accessed on 16 December 2025)	60–100 m	2014–2016
Log conflict density (ConflictDens_log, CDl)	Based on kernel density from conflict-related places; transformation $\log_{10}(\text{ConflictDens} + 10^{-6})$ was applied due to strong concentration near zero.	CNMH (2022) [42]	https://geoportal-de-datos-abiertos-cnmh-cnmh.hub.arcgis.com/datasets/285a0cfe6aa34f65ab49c95aee298d0e_1/about (accessed on 16 December 2025)	30 m	2000–2024
Distance to agricultural areas (DistAgriculture, DA)	Euclidean distance to agriculture areas (km) was computed as the straight-line distance from each agriculture areas to the nearest páramo boundary.	IDEAM (2021) [43]	https://www.colombiaenmapas.gov.co/?e=-90.24363391601412,-5.572398896778716,-55.74656360352328,13.859268426770145,4686&b=igac&l=881&u=0&t=4302&servicio=881 (accessed on 16 December 2025)	60–100 m	2018
Precipitation (P)	Multi-annual accumulated precipitation from TerraClimate.	TerraClimate (2024) [44]	https://www.climatologylab.org/terraclimate.html (accessed on 16 December 2025)	4000 m	2000–2022
Max Temperature (°C) (T)	Multi-year mean of maximum temperature from TerraClimate.	TerraClimate (2024) [44]	https://www.climatologylab.org/terraclimate.html (accessed on 16 December 2025)	4000 m	2000–2022
Elevation (E)	Altitude above sea level.	IGAC (2011) [45]	https://www.colombiaenmapas.gov.co/?e=-82.66306750976614,-1.8784752954619761,-65.83201282227061,11.877955613394604,4686&b=igac&u=0&t=23&servicio=159 (accessed on 16 December 2025)	30 m	2011
NDVI (NDVI)	Median normalized difference vegetation index computed from Landsat 5, 7, 8, and 9.	Processing was performed in Google Earth Engine using code developed by the authors of this study	https://code.earthengine.google.com/b14e1f08d76eb28c45e35148517f485d (accessed on 16 December 2025)	30 m	2000–2024
Human footprint (HFP)	Degree of impact of human activities (0 = no impact, 100 = maximum impact).	Correa et al. (2020) [46]	https://geonetwork.humboldt.org.co/geonetwork/srv/spa/catalog.search#/metadata/e29b399c-24ee-4c16-b19c-be2eb1ce0aae (accessed on 16 December 2025)	300 m	1990–2015
Protected areas (PAs)	Boundary of protected areas in Colombia.	RUNAP (2025) [39]	https://storage.googleapis.com/pnn_geodatabase/runap/latest.zip (accessed on 16 December 2025)	60–100 m	2025

2.2.3. Spatial Analysis

We based the spatial analysis on the páramo Fire Atlas, which served as the dependent variable. Because our objective was to analyze broad-scale patterns in fire frequency rather than pixel-level fire occurrence, we did not convert the annual burned-area layers into a binary burned/unburned dataset. Rather, to better capture meaningful spatial gradients in fire activity, we aggregated the data to a 500 × 500 m grid and calculated, for each cell, the cumulative percentage of burned area over the 2000–2022 period. To account for repeated burning, we used the burn-count layer of the Fire Atlas. Only 15.5% of the burned area experienced more than one fire during the study period, and all repeated burns were included in the cumulative burned-area values assigned to each grid cell. While this aggregation does not alter the inherent stochasticity of fire events themselves, it reduces fine-scale variability and produces a more robust metric of fire frequency that aligns with the spatial resolution of the explanatory variables. All explanatory variables were resampled to the same 500 × 500 m resolution using bilinear interpolation to ensure consistency across datasets.

To assess redundancy among predictors, we computed pairwise Pearson correlation coefficients, a widely used approach for detecting linear dependencies that contribute to multicollinearity [47], applying a ±0.65 threshold to exclude one variable from each highly correlated pair, which indicated that elevation and conflict density were correlated with maximum temperature (−0.83) and distance to buildings (−0.69), respectively. Our use of Pearson correlation was intended solely as a diagnostic of linear redundancy among predictors and not as an assessment of predictor–response relationships. Given that exploratory analyses revealed nonlinear relationships between predictors and burned area, we opted not to use traditional parametric approaches such as linear or logistic regression, which rely on assumptions of linearity [48–50].

Instead, we developed a predictive model using Random Forest, a non-parametric ensemble learning method well suited to capture nonlinear interactions and complex predictor–response relationships [51]. This approach enabled us to evaluate how biophysical and anthropogenic variables contribute to the spatial patterns of burned area. Variable importance was assessed using the permutation importance metric, which measures the increase in prediction error when a variable's values are randomly permuted. We report this metric as the percentage increase in mean squared error (%IncMSE). To further explore predictor effects, we generated partial dependence plots to describe the form of the predictor–response relationship between each variable and burned area [52]. These plots estimate the average marginal effect of a single variable on the response while holding all others constant, thereby isolating its contribution to the model's prediction. The RF model was parameterized with 500 trees and three variables considered at each split. All analyses were performed in R version 4.5.2, using the terra package for spatial analysis [53] and the randomForest [51] and corrplot packages for statistical analysis [54]. To evaluate whether model errors exhibited spatial dependence, we assessed spatial autocorrelation in the Random Forest residuals using Moran's I calculated on a spatially random subset of 10,000 observations.

3. Results

3.1. Burned Area

Figure 3 shows the accumulated burned area (%) for each Colombian páramo unit from 2000 to 2022, reflecting how fire activity has differed among páramos over the study period. Reburning was relatively uncommon across Colombian páramos: only 15.5% of the total burned area showed evidence of more than one fire event. Burned area distribution varied widely among the three cordilleras: the Eastern cordillera recorded the largest proportion (8.9%), the Central reached intermediate levels (3.5%), and the Western was least affected (0.5%), with near-zero values in páramo units such as Citará and El Duende (Tables A1 and A2). These results underscore the heterogeneous distribution of burned areas in Colombian páramos, with marked contrasts both among and within cordilleras (Figure A3).

Within this general pattern, the Eastern Cordillera stands out with the most burned páramos units, especially those near major cities—such as Tota-Vijagual (34),

https://doi.org/10.3390/fire9030095

Cruz Verde–Sumapaz (9), and Altiplano Cundiboyacense (2)—and in binational systems like Perijá (36), where one-third of its area has burned. In the Central Cordillera, the Chiles–Cumbal páramo (5) shows the highest impact, with one-fifth of its surface burned during the study period.

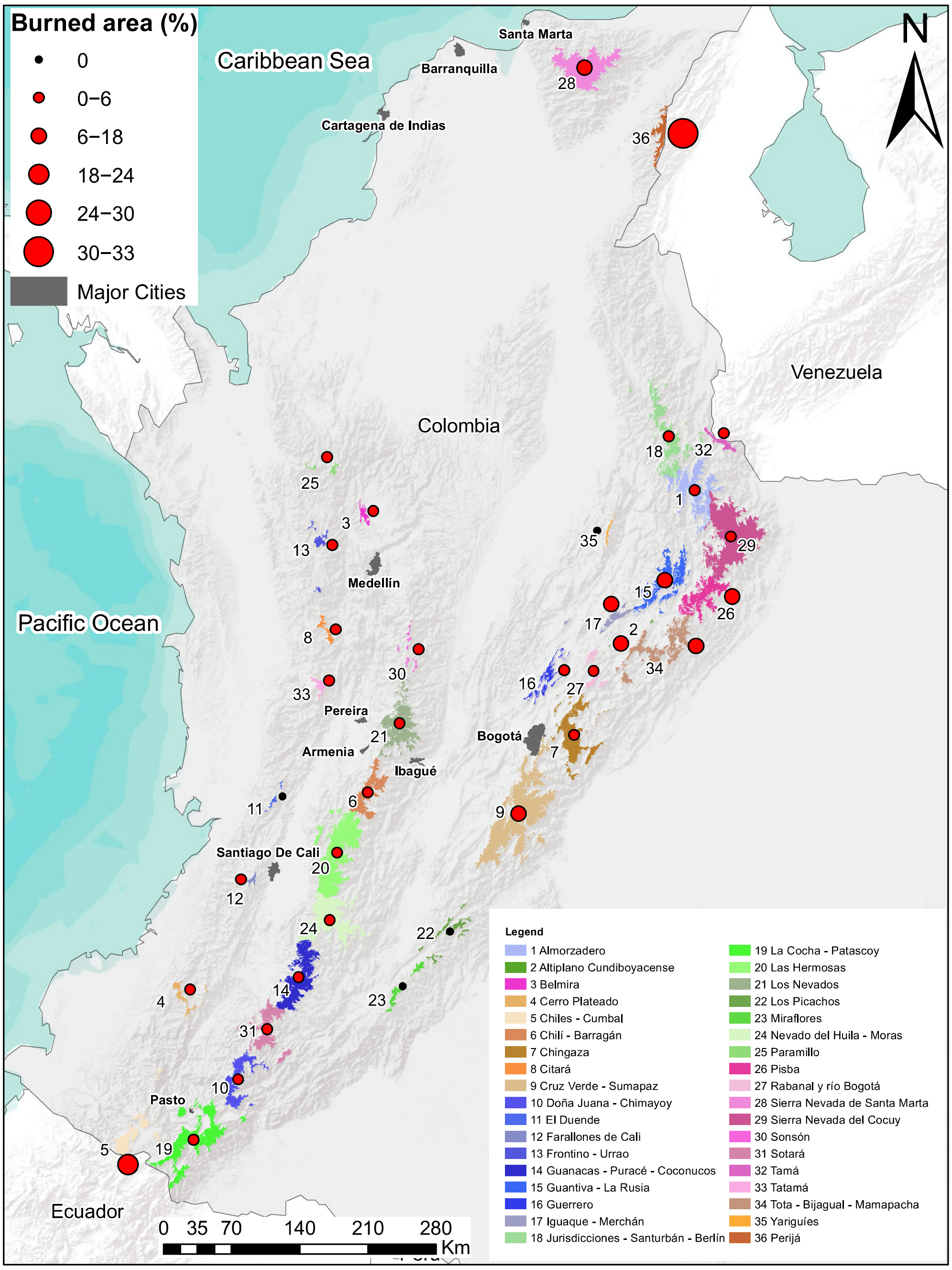

Figure 3. Percentage of burned area of each páramo unit in Colombia from 2000 to 2022 based on data from the páramo Fire Atlas [13]. Each páramo unit is numbered from 1 to 36 to facilitate its location on the map.

Burned area was strongly concentrated in a limited subset of páramo units. The ten units with the greatest burned extent accounted for 84% of the total area burned across all páramos over the 22-year study period. These same units also exhibited the highest burned proportions, demonstrating a tight correspondence between absolute burned extent and the relative intensity of burning within individual páramos (see Figure 4). This pattern

https://doi.org/10.3390/fire9030095

indicates that fire effects are both extensive and disproportionately focused in systems where large portions of the landscape have burned at least once.

Regarding the spatial distribution of burned and unburned areas relative to protection status, all burned areas overlapped at least partially with RUNAP boundaries. Partitioning each unit into the four categories (Burned + PA, Burned − PA, Unburned + PA, Unburned − PA) and examining their normalized composition in ascending order of burned proportion revealed pronounced differences among the most influenced páramos (see Figure 4). In every unit, unburned areas outside PAs accounted for the largest share of the landscape, while the proportion of burned area outside PAs increased steeply in páramos with the highest fire incidence (e.g., Perijá, Chiles–Cumbal, Tota–Bijagual–Mamapacha). Conversely, burned area within PAs consistently represented only a small fraction of each unit, and unburned area within PAs showed relatively little variation across páramos. Collectively, these patterns indicate that although burned and protected areas do overlap, the overall composition of fire impacts is dominated by both unburned and burned areas located outside protected boundaries.

At the national level, the total burned area was slightly higher within protected areas than outside them, but this pattern did not consistently emerge at the scale of individual páramo units. Once normalized by available surface area, the proportions burned inside and outside protected areas were highly variable and exhibited no statistically significant differences (W = 546, p = 0.716) (Figure A2 and Table A1).

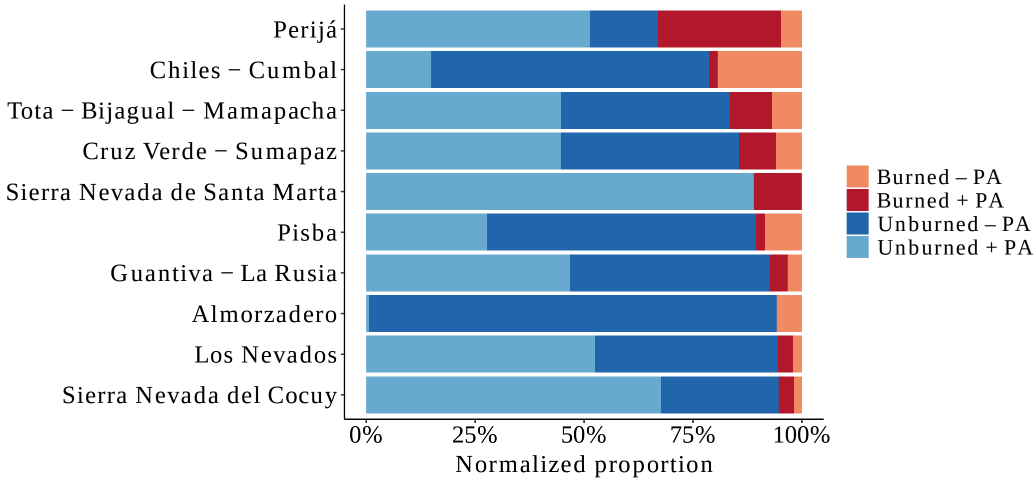

Figure 4. Normalized proportion of burned and unburned areas inside and outside protected areas for the ten páramo units with the greatest total burned extent (2000–2022). Bars are ordered by increasing burned proportion. Categories correspond to burned inside protected areas (Burned + PA), burned outside protected areas (Burned − PA), unburned inside protected areas (Unburned + PA), and unburned outside protected areas (Unburned − PA). These ten units together account for 84% of the total burned area across all páramo units.

3.2. Drivers of Burned Area Across the Páramo Ecosystem

Our model provided a robust representation of spatial variation in burned area across páramo units, successfully capturing broad spatial patterns in fire occurrence and offering a reliable foundation for interpreting the influence of biophysical and human-related factors. The predictor relationships embedded in the Random Forest framework showed substantial explanatory and predictive value, with moderate model performance (out-of-bag mean squared residual = 137.7; RMSE = 11.7; explained variance = 54.3%). Although residuals exhibited significant positive spatial autocorrelation (Moran's I = 0.099, $p < 0.001$), this pattern is expected in large, environmentally heterogeneous landscapes such as the páramos, where biophysical gradients and human activities are strongly clustered in space. Overall, the model remains well suited for identifying broad-scale drivers of fire occurrence and characterizing regional patterns in páramo fire dynamics.

Figure 5 presents the ranked importance of each predictor variable (%IncMSE). Precipitation emerged as the most influential driver in burned area within the páramo region, followed by anthropogenic variables such as distance to buildings, distance to agricultural areas, and the human footprint index, and NDVI ranked fifth in importance. Variables such as distance to forests, temperature, distance to roads, and protected area category exhibited lower importance in explaining burned area.

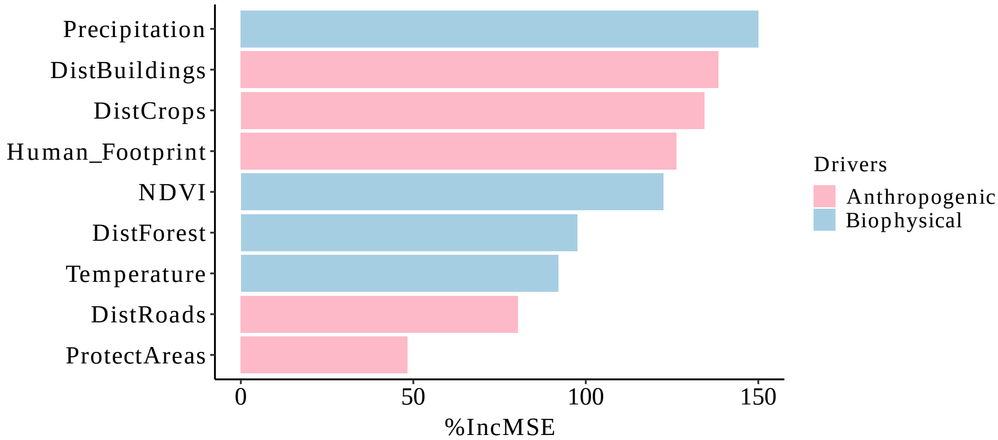

Figure 5. Variable importance of biophysical and anthropogenic predictors for burned area. Variable importance was assessed using the percentage increase in mean squared error (%IncMSE) from the Random Forest model. Predictors are grouped by category (biophysical and anthropogenic). The abbreviated variable names are in Table 1.

3.2.1. Biophysical Variables

Annual precipitation was the strongest predictor of burned area variability. Partial dependence plots (Figure 6) show that the burned area is 75% higher under drier conditions, particularly when precipitation falls below 1500 mm/year (see Table A3) compared to wetter areas. The burned area is also 80% higher in areas with mean temperatures above 16°C, relative to cooler páramo zones (<12°C). Vegetation greenness (NDVI) shows a hump-shaped response: areas with intermediate density (0.13–0.20) nearly double the predicted burned area compared to sparsely vegetated (<0.1) or densely forested areas (>0.25).

Although distance to forests and proximity to roads ranked low in the model results, they still influenced burned area (Figure 6). Burned area increased at distances greater than 2 km from forest and roads, which is consistent with the NDVI pattern showing that areas with denser forest cover experienced fewer fires.

3.2.2. Human Pressure

Agricultural areas and distances to buildings increase the probability of burned areas (Figure 6). Burned area peaks within the first two kilometers (agriculture) and nine kilometers (buildings) of these features and declines with distance, although secondary peaks emerge at greater distances (see Table A3). Both variables were strong predictors of burned area, and their partial dependence curves showed average predicted burned-area values ranging between 4% and 16%.

For buildings, predicted burned area increased sharply beyond 8 km from built structures. For the human footprint index (0 = null impact; 100 = maximum impact), predicted burned area was highest at low-impact values (0–20) (see Table A3) and then declined steadily to approximately 30. Beyond this threshold, variability was minimal, yielding a relatively flat pattern that appears counterintuitive given the generally higher human influence at those levels.

For the protected-area categories, predicted burned area differed only marginally between protected and unprotected regions. Within protected areas, however, zones under medium and high restriction exhibited lower predicted burned area than those under low restriction. This pattern is consistent with the fact that stricter protection categories restrict activities such as grazing, pasture renovation, and the use of fire as a management tool, thereby reducing potential ignition sources. In contrast, low-restriction areas typically permit human use and easier access, conditions that elevate fire likelihood. Overall, this variable exerted a modest influence in the model, with predicted burned-area values ranging only from 0% to 7%.

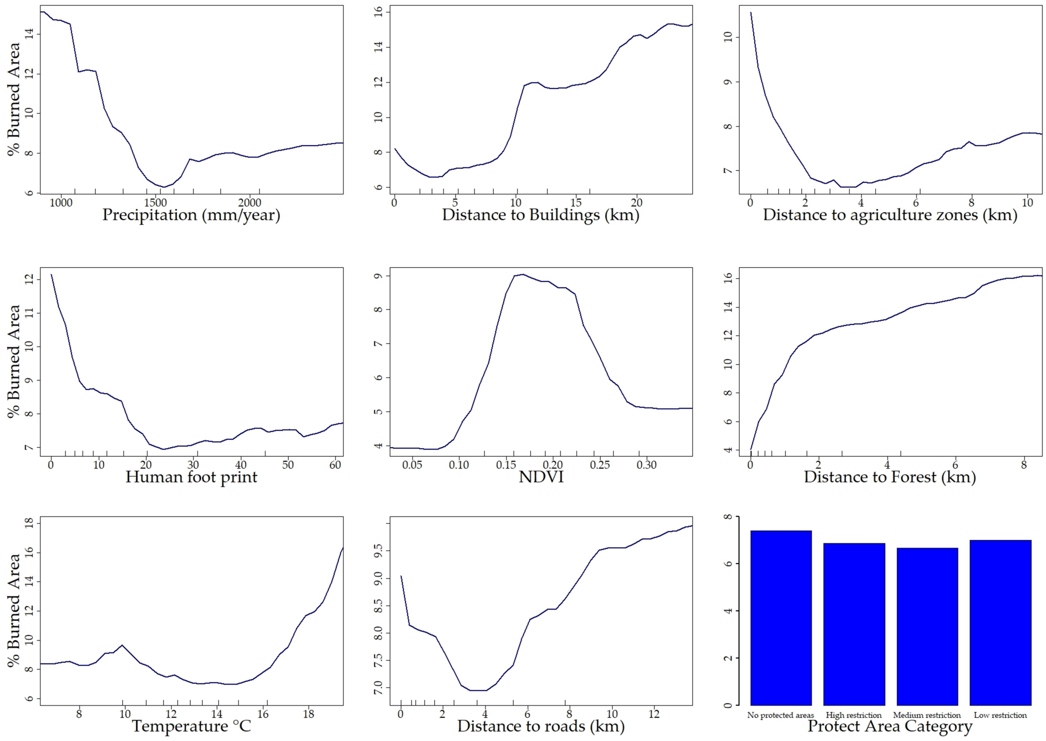

Figure 6. Partial dependence plots for the main predictors of burned area in Colombian páramos. The x-axes display predictor values, with vertical tick marks denoting deciles of their empirical distributions. The y-axes indicate the predicted percentage of area burned while holding all other variables constant. Together, these plots illustrate the marginal influence of each predictor on burned area as estimated by the Random Forest model. Thresholds are in Table A3.

4. Discussion

4.1. Biophysical and Anthropogenic Drivers of Fire Patterns

This study shows that fire dynamics in páramo ecosystems result from the combined influence of anthropogenic and biophysical drivers. While human activities have been widely recognized as the main source of ignitions [8,26], our findings demonstrate that biophysical variables also play a critical role in shaping spatial fire patterns. Likewise, our analysis of burned areas across Colombian páramos over the past 22 years reveals strong spatial heterogeneity. Burned area exhibits strong regional differences, with the Eastern Cordillera—characterized by the highest fire frequency and total burned extent—clearly standing out as the region with the most concentrated fire activity.

Contrary to our initial hypothesis, where we expected human variables to explain most of the spatial variability in burned area, the RF model revealed that mean annual precipitation is the most influential predictor. Drier areas exhibit higher burned areas, but the relationship is not linear; instead, precipitation shows a critical threshold, with burned area increasing sharply in regions receiving less than 1500 mm of annual rainfall. This pattern aligns with findings from other Andean ecosystems, where rainfall preceding the fire season and during dry periods regulates fire dynamics [25,26,35]. Overall, these results highlight how moisture availability, interacting with fuel loads and human activities, shapes fire patterns in high-altitude landscapes.

The second-most important biophysical predictor was NDVI, which explained a substantial share of burned area variability. The model revealed a unimodal relationship between vegetation greenness (NDVI 0.15–0.25) and burned area, indicating that areas with intermediate vegetation density—such as grasslands dominated by clumped grasses in a continuous layer [55]—are the most susceptible to fire. These grasslands dominate much of the páramo landscape, providing the primary fuel that drives fire patterns [19]. This pattern reflects fuel availability thresholds: low NDVI areas lack sufficient continuous biomass to sustain fire, whereas high NDVI areas usually retain more moisture, which limits fire spread [56]. These areas are generally occupied by Andean forests or shrubs [2]. Although the most important variable is biophysical, human pressures have a strong impact, shaping ignition patterns and reinforcing fire pressure across páramos units.

Anthropogenic factors exerted a strong influence on burned area [8]. Proximity to buildings and croplands was closely linked to higher burned area. This pattern reflects greater accessibility for ignition sources, both intentional and accidental. Intentional uses include agricultural expansion, burning to promote regrowth for livestock, deforestation, and the clearing of woody vegetation [19,26]. Accidental ignitions and vandalism have also been reported [26,57]. Historically, páramos have been shaped by the combined influence of fire and grazing as part of their land-use history [8,19,26], as well as domestic fuel use and charcoal production [16]. Cultural practices and local beliefs promote the use of fire, such as burning páramo vegetation during dry periods under the assumption that smoke induces cloud formation and rainfall [16,27]. More recently, demographic pressures, including population growth, increased tourism and the proximity of urban centers, have been linked to heightened fire pressure [20,26,32,58].

4.2. Climate, Land-Use Pressures, and Future Fire Regimes

Our results confirm that burned areas in páramo units do not occur randomly in space or time but rather emerge from predictable dynamics within coupled human–natural systems. Looking ahead, projected reductions in precipitation and rising temperatures are likely to increase flammability, while expanding agriculture, grazing, urban growth, and rising tourism may intensify human pressures [21,32,58]. Taken together, these trends suggest that fire patterns in páramo ecosystems are likely to increase in the future, driven by the combined effects of climate change and evolving socio-economic dynamics. This highlights the urgent need for targeted, adaptive management strategies.

4.3. Fire Recurrence, Fuel Continuity, and Ecological Implications

Our analysis focused on cumulative burned area over the 22-year period, but a minority of pixels (15.5% of the burned area) experienced more than one fire event. These repeated-burn areas are ecologically distinct from those that burned only once, as páramo vegetation typically requires several years to recover enough biomass to sustain another fire [59]. Multiple burns therefore indicate locations where ignitions recur and where fuel accumulates rapidly enough to support repeated fire events—a pattern consistent with the spatial clustering of human activities documented in several páramo regions [5,7]. Although our Random Forest model used cumulative burned extent rather than individual fire events, the presence of pixels with two or more burns suggests that the drivers of repeated fires may differ from those of single-burn areas, and that fire intensity, vegetation recovery, and fuel continuity may interact differently in these locations. Incorporating fire-frequency metrics into future analyses would help distinguish areas where fire acts as a recurrent disturbance from those where it occurs as a singular event, improving understanding of how fuel dynamics, vegetation structure, and land-use practices shape fire regimes in páramo ecosystems.

4.4. Fire Intensity, Fuel Structure, and Flammability Constraints

An important complementary dimension is fire intensity. While burned-area metrics capture the spatial footprint of fire, they do not reflect the energy released, the depth of soil heating, or the severity of impacts on vegetation and soils. In páramo ecosystems, low-intensity fires may burn aboveground biomass without consuming tussock bases, enabling relatively rapid regrowth [1,20], whereas high-intensity events can lead to deep organic-soil combustion, extensive root mortality, and persistent alterations to vegetation structure [1,28]. Fuel accumulation thus affects not only the probability that fires will occur and spread but also their potential intensity and ecological consequences.

A second limitation of our analysis is the absence of species-level flammability traits, which are not currently available at national scales [26]. In high-Andean grasslands, fire behavior is governed less by the intrinsic flammability of individual species and more by the structure and arrangement of fine fuels—dense tussock grasses, senescent biomass, shallow organic layers, and litter-like material that together determine continuity, combustibility, and residence time [26,28]. Although in some fire-prone ecosystems frequent low-intensity burns can reduce fine fuels and mitigate extreme events, repeated burning in páramos often slows vegetation recovery and can degrade organic soils, making these dynamics less applicable to these high-mountain systems. Similar patterns have been documented in other high-mountain grassland systems—such as the Andean puna—where fuel continuity, fine-fuel accumulation, and moisture constraints strongly shape fire patterns [10].

Consequently, NDVI and vegetation-type variables acted as coarse proxies for fuel availability and cannot resolve fine-scale variation in flammability or fire intensity [26]. Because our analysis focused on burned extent rather than intensity, inflammability, or structural fuel properties, some spatial patterns—particularly in areas with recurrent burns or extensive continuous fuel beds—may reflect differences in fire behavior that the model cannot capture. Incorporating fire-severity indicators (e.g., spectral severity indices, soil thermal impacts, vegetation mortality patterns) and, where feasible, functional-trait or flammability data, would provide a more mechanistic understanding of how vegetation structure, fuel dynamics, and ignition pressures jointly shape fire regimes and their ecological outcomes in páramo landscapes.

4.5. Effectiveness of Protected Areas

Despite the presence of national fire-suppression policies—including the explicit prohibition of burning in páramo ecosystems (Law 2111 of 2021; Decree 1076 of 2015; Resolution 358 of 2024)—our results show that legal protection, on its own, does not consistently reduce burned area. Although the national total of burned area was slightly higher inside protected areas, this pattern largely reflects the extensive size of several protected páramos rather than a systematic tendency for fires to concentrate within protected boundaries. Once normalized by available area, burned proportions exhibited high variability and broad overlap across units, aligning with the absence of statistically significant differences reported in the Results. These findings indicate that the effectiveness of protection measures is strongly conditioned by local socio-ecological contexts rather than by protection status as an isolated factor. Units under medium- and high-restriction categories displayed somewhat lower burned proportions, but the differences were modest and not systematic.

Furthermore, the effectiveness of the National System of Protected Areas (SINAP) is hindered by institutional constraints: only about 14% of the national environmental budget is allocated to SINAP, and its management effectiveness index is approximately 65% [60]. These institutional limitations, together with persistent local land-use practices involving fire, help explain the continued occurrence of fire events even within protected páramo areas. Taken together, these patterns underscore that formal protection, by itself, does not guarantee effective fire prevention. Its effectiveness ultimately hinges on enforcement capacity, local legitimacy, and the degree to which legal frameworks align with the socio-ecological realities operating on the ground.

4.6. Implications for Fire Management and Policy

It is crucial to recognize these predictable dynamics, as they enable the design of targeted interventions that address the most influential drivers of fire risk. These insights highlight the urgent need for integrated and spatially explicit fire management strategies in páramo ecosystems. Key actions include implementing early warning systems during dry seasons and promoting sustainable, fire-free alternatives for pasture renewal where feasible (including mechanical clearing of senescent biomass and rotational grazing systems). Monitoring vegetation transitions is essential not for directly preventing fuel accumulation, but for identifying where continuous, fire-prone fuels are forming and for informing decision-making. This information allows managers to prioritize preventive actions—such as establishing early-intervention zones, designing fuel-disruption mosaics, or implementing community-based surveillance—to reduce the likelihood of extreme fire events in areas where fuels accumulate atypically.

However, the implementation of such preventive and adaptive measures requires an Integrated Fire Management (IFM) framework, which Colombia currently lacks. Existing regulations focus almost exclusively on fire suppression (Law 2111 of 2021; Decree 1076 of 2015; Resolution 358 of 2024), limiting the extent to which proactive strategies and local knowledge can be incorporated. As a consequence, the customary practices and observations of communities with long-standing relationships with fire—such as local indicators used to anticipate seasonal flammability, experience-based norms that help prevent accidental ignitions, or traditional grazing and vegetation-use practices—are rarely integrated into formal management. Incorporating this traditional ecological knowledge into scientifically grounded IFM planning would not supplant evidence-based policy; rather, it would enrich it by providing context-specific insights that improve early detection, risk anticipation, and community engagement. Such integration is particularly critical in páramo landscapes, where fire dynamics are closely intertwined with social practices and where suppression-only approaches have historically shown limited effectiveness [26].

Beyond prevention and control, it is urgent to understand how fire affects biodiversity and ecosystem services, given the limited knowledge available. Addressing this gap is critical to strengthen fire prevention, enhance ecosystem resilience, and align conservation efforts with local practices.

Author Contributions: Conceptualization, J.J.D.-T. and S.H.; methodology, J.J.D.-T. and S.H.; formal analysis, J.J.D.-T.; investigation, J.J.D.-T., L.O.-C., S.H. and S.T.A.; data curation, J.J.D.-T. and L.O.-C.; software, J.J.D.-T.; writing—original draft preparation, J.J.D.-T.; writing—review and editing, J.J.D.-T., L.O.-C., S.H. and S.T.A.; supervision, S.H. and S.T.A. All authors have read and agreed to the published version of the manuscript.

Funding: S.H., J.J.D.-T., L.O.-C. acknowledge support from the Max Planck Tandem group program. S.H. acknowledges support from Universidad del Rosario within the program of Fondos de arranque.

Institutional Review Board Statement: Not applicable.

Informed Consent Statement: Not applicable.

Data Availability Statement: All data used in this study is publicly available. Links to each dataset are provided in Table 1.

Acknowledgments: The author sincerely thanks his family, especially his wife and daughter, for their support and encouragement throughout this research. During the preparation of this manuscript, the authors used ChatGPT (OpenAI, GPT-5) to assist in language editing and improving the clarity of expression. The authors reviewed and revised all AI-generated suggestions and take full responsibility for the content of this publication.

Conflicts of Interest: The authors declare no conflicts of interest.

Abbreviations

The following abbreviations are used in this manuscript:

RUNAP	Registro Único de Areas Protegidas
SINA	Sistema Nacional Ambiental
SINAP	Sistema Nacional de Areas Protegidas

Appendix A

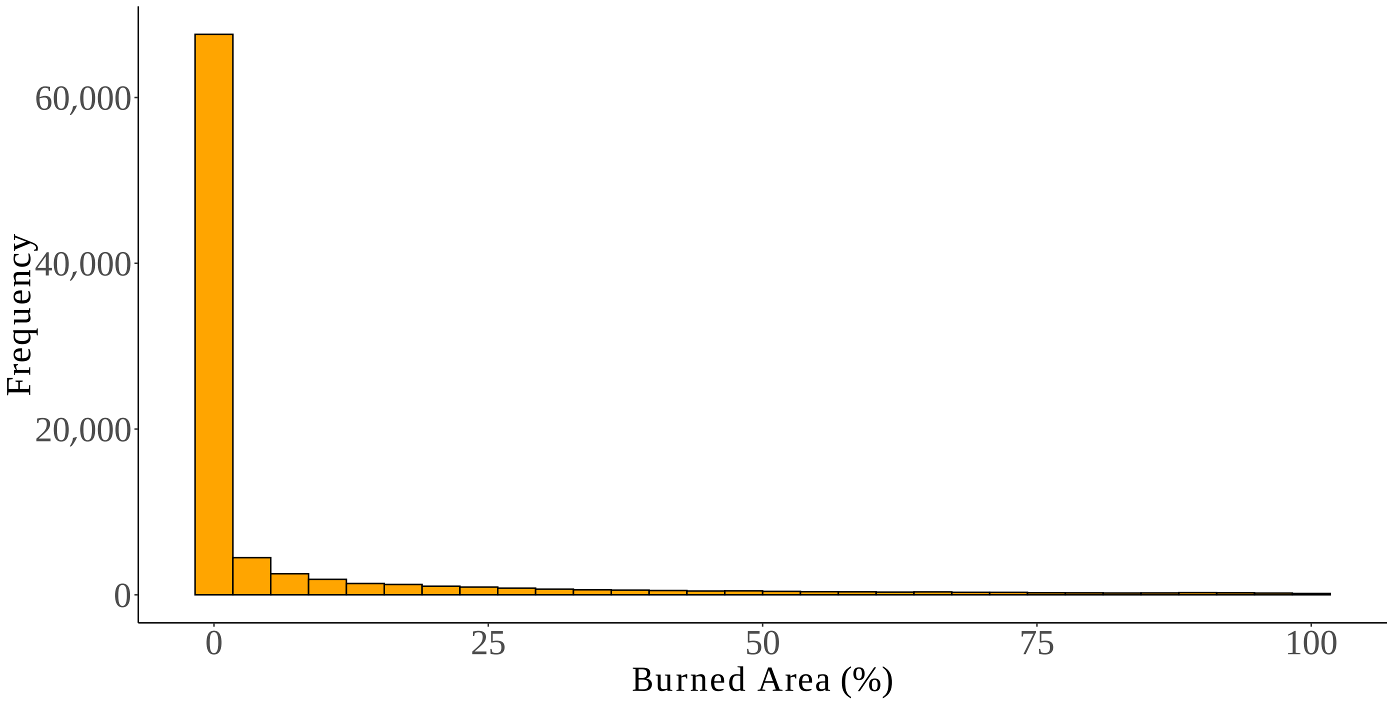

Figure A1. The frequency distribution of burned area percentages across all páramo units reveals a strong right-skewed pattern. Most observations correspond to less than 5% of burned area, while only a small proportion exceed 25%. This indicates that, although fire events are widespread, they tend to affect limited portions of the landscape. The long tail of the distribution suggests that extensive burns are rare but occur occasionally.

Table A1. Páramo units grouped by Cordillera, with burned and protected proportions.

Páramo	% Burned (Páramo)	% Total Burned	% Protected Area	Cordillera
Belmira	2.23	0.13	100.00	Western
Cerro Plateado	0.55	0.05	18.22	
Frontino-Urrao	0.35	0.03	84.49	
Paramillo	0.04	0.002	99.88	
Farallones de Cali	0.02	0.0005	100.00	
Tatamá	0.01	0.0007	100.00	
Citará	0.00	0.0003	56.11	
El Duende	0.00	0	39.77	
Chiles-Cumbal	21.34	6.24	16.99	Central
Los Nevados	5.49	3.89	56.03	
Nevado del Huila-Moras	4.06	3.59	78.22	
Guanacas-Puracé-Coconucos	2.81	2.09	24.96	
Las Hermosas	2.62	3.08	65.08	
Chilí-Barragán	1.80	0.82	35.73	
La Cocha-Patascoy	0.82	0.68	34.98	
Sotará	0.76	0.34	42.05	
Sonsón	0.20	0.010	43.39	
Doña Juana-Chimayoy	0.13	0.05	50.85	
Perijá	33.11	5.97	79.67	Eastern
Tota-Bijagual-Mamapacha	16.59	10.73	54.60	
Altiplano Cundiboyacense	16.13	0.13	11.89	
Cruz Verde-Sumapaz	14.44	25.87	53.23	
Sierra Nevada de Santa Marta	11.00	10.07	100.00	
Pisba	10.56	5.14	29.86	
Guantiva-La Rusia	7.34	4.10	50.82	
Iguaque-Merchán	6.21	0.80	54.27	
Almorzadero	5.86	4.19	0.64	
Sierra Nevada del Cocuy	5.33	7.80	71.27	
Rabanal y río Bogotá	5.22	0.62	68.56	
Guerrero	3.78	0.55	85.34	
Jurisdicciones-Santurbán-Berlín	3.31	2.17	43.00	
Chingaza	1.34	0.84	81.53	
Tamá	0.12	0.012	75.03	
Los Picachos	0.00	0	88.20	
Miraflores	0.00	0	84.57	
Yariguíes	0.00	0	99.36	

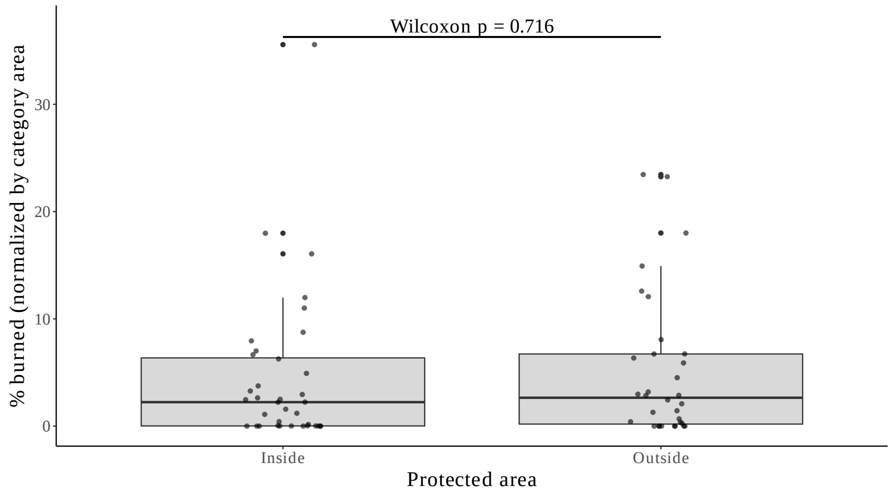

Figure A2. Normalized burned area inside and outside protected areas (PAs; % relative to the available area in each category). Boxplots display the distribution of páramo-level values, paired within complexes to account for variation in total size. Statistical comparison using the Wilcoxon signed-rank test revealed no significant differences between inside and outside fractions (two-sided $p = 0.716$; one-sided test for inside < outside $p = 0.371$).

Table A2. Distribution of burned area by cordillera.

Cordillera	Total Area (ha)	Burned Cells	% Burned
Central	1,013,731	35,121	3.46
Eastern	1,490,635	133,452	8.95
Western	77,968	362	0.46

Table A3. Threshold values marking changes in the relationship between each predictor and burned area, as derived from the Random Forest partial dependence plots (see Figure 6). Breakpoints were identified using the Bai–Perron multiple structural change method, with the optimal number of change points determined by the Bayesian Information Criterion. Reported values reflect the estimated predictor levels at which the response slope changes, expressed in the original units of each variable (excluding categorical predictors such as ProtectedAreas).

Variable	Thresholds
DistForest	1.72
Temperature	17.08
Precipitation	1577.41
DistBuildings	9.60
DistRoads	5.60
DistAgriculture	2.14
NDVI	0.14
ProtectAreas	–
Human Footprint	20.50

Comparison between Cordilleras

Kruskal–Wallis tests based on normalized values (% burned area relative to total páramo area) indicated significant differences among cordilleras (H = 9.18, p = 0.0101). Post hoc pairwise Mann–Whitney tests revealed that the Western cordillera differed significantly from both the Central (p = 0.0044) and Eastern (p = 0.0123), whereas no significant difference was detected between Central and Eastern cordilleras (p = 0.2212).

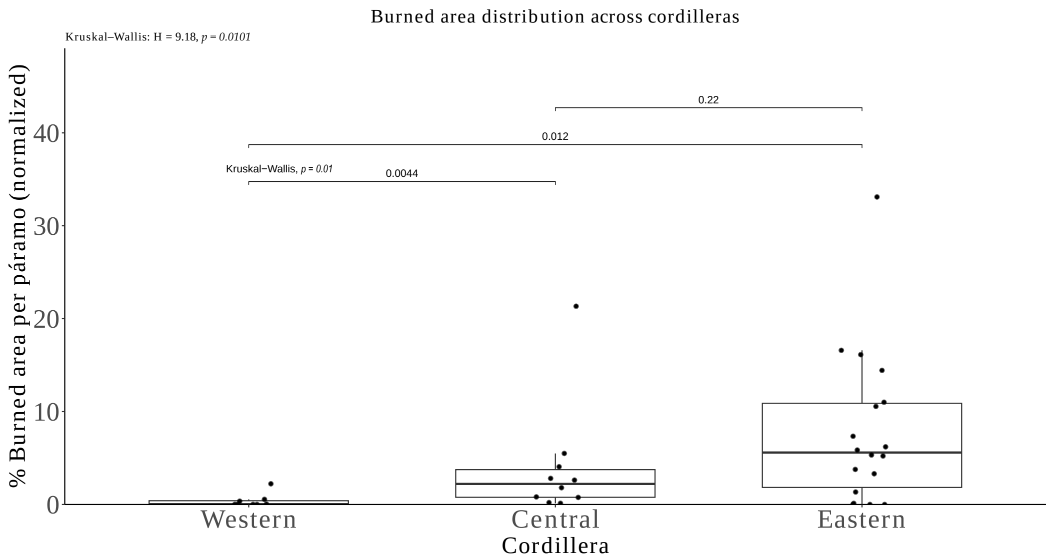

Figure A3. Boxplots of burned area normalized by páramo size (percent of each páramo's area burned) across the Western, Central, and Eastern Cordilleras. A Kruskal–Wallis test detected differences among cordilleras (H = 9.18, $p = 0.010$). Post hoc pairwise Mann–Whitney U tests showed Western < Central ($p = 0.0044$) and Western < Eastern ($p = 0.012$), whereas Central vs. Eastern was not significant ($p = 0.22$). Points represent individual páramos units.

References

1. Ramsay, P.M.; Oxley, E.R. Fire temperatures and postfire plant community dynamics in Ecuadorian grass páramo. *Vegetatio* **1996**, *124*, 129–144. [CrossRef]

2. Hofstede, R.G.; Llambí, L.D. Plant Diversity in Páramo—Neotropical High Mountain Humid Grasslands. In *Encyclopedia of the World's Biomes*; Elsevier: Amsterdam, The Netherlands, 2020; Volumes 1–5. pp. 362–372. [CrossRef]
3. Madriñán, S.; Cortés, A.J.; Richardson, J.E. Páramo is the world's fastest evolving and coolest biodiversity hotspot. *Front. Genet.* **2013**, *4*, 192. [CrossRef]
4. Bond, W.J.; Woodward, F.I.; Midgley, G.F. The global distribution of ecosystems in a world without fire. *New Phytol.* **2005**, *165*, 525–538. [CrossRef]
5. Chuncho, C.; Chuncho, G. Páramos del Ecuador, Importancia y Afectaciones: Una Revisión. 2019. Available online: https://www.researchgate.net/publication/344180955 (accessed on 16 December 2025).
6. Sarmiento, P.C.E.; Cadena, V.C.E.; Sarmiento, G.M.V.; Zapata, J.J.A. *Aportes a la Conservación Estratégica de los Páramos de Colombia: Actualización de la Cartografía de los Complejos de Páramo a Escala 1:100.000*; Instituto de Investigación de Recursos Biológicos Alexader von Humboldt: Bogotá, Colombia, 2013; p. 87.
7. Borrelli, P.; Armenteras, D.; Panagos, P.; Modugno, S.; Schütt, B. The implications of fire management in the andean paramo: A preliminary assessment using satellite remote sensing. *Remote Sens.* **2015**, *7*, 11061–11082. [CrossRef]
8. Le Stradic, S.; Alvarado, S.T.; Ríos, O.V.; Silveira, F.A.O. Fire Ecology on Megadiverse Montane Grasslands. In *Fire in the South American Ecosystems*; Springer: Cham, Switzerland, 2025; pp. 187–211. [CrossRef]
9. Keating, P.L. Fire ecology and conservation in the high tropical Andes: Observations from northern Ecuador. *J. Lat. Am. Geogr.* **2007**, *6*, 43–62. [CrossRef]
10. Young, B.E.; Young, K.R.; Josse, C. *Vulnerability of Tropical Andean Ecosystems to Climate Change*. In *Climate Change and Biodiversity in the Tropical Andes*; Herzog, S.K., Martínez, R., Jørgensen, P.M., Tiessen, H., Eds.; Inter-American Institute for Global Change Research (IAI): Ciudad del Saber, Edificio; Scientific Committee on Problems of the Environment (SCOPE): Paris, France, 2011; pp. 1–18.
11. White, S. Grass páramo as hunter-gatherer landscape. *Holocene* **2013**, *23*, 898–915. [CrossRef]
12. Bush, M.B.; Rozas-Davila, A.; Raczka, M.; Nascimento, M.; Valencia, B.; Sales, R.K.; McMichael, C.N.; Gosling, W.D. A palaeoecological perspective on the transformation of the tropical Andes by early human activity. *Philos. Trans. R. Soc. Lond. B. Biol. Sci.* **2022**, *377*, 20200497. [CrossRef] [PubMed]
13. Obando-Cabrera, L.; Díaz-Timoté, J.J.; Bastarrika, A.; Celis, N.; Hantson, S. The Paramo Fire Atlas: Quantifying burned area and trends across the Tropical Andes. *Environ. Res. Lett.* **2025**, *20*, 054019. [CrossRef]
14. Espinoza, I.G.; Franco-Gaviria, F.; Castañeda, I.; Robinson, C.; Room, A.; Berrío, J.C.; Armenteras, D.; Urrego, D.H. Holocene Fires and Ecological Novelty in the High Colombian Cordillera Oriental. *Front. Ecol. Evol.* **2022**, *10*, 475. [CrossRef]
15. Vásquez, D.L.; Balslev, H.; Sklenář, P. Human impact on tropical-alpine plant diversity in the northern Andes. *Biodivers. Conserv.* **2015**, *24*, 2673–2683. [CrossRef]
16. Horn, S.P.; Kappelle, M. Fire in the páramo ecosystems of Central and South America. In *Tropical Fire Ecology*; Springer: Berlin/Heidelberg, Germany, 2009; pp. 505–539. ._18 [CrossRef]
17. League, B.L.; Horn1, S.P. A 10 000 year record of Páramo fires in Costa Rica. *J. Trop. Ecol.* **2000**, *16*, 747–752. [CrossRef]
18. Carrión-Paladines, V.; Correa-Quezada, L.; Valdiviezo Malo, H.; Zurita Ruáles, J.; Pereddo Tumbaco, A.; Zambrano Pisco, M.; Lucio Panchi, N.; Jiménez Álvarez, L.; Benítez, M.; Loján-Córdova, J. Exploring the ethnobiological practices of fire in three natural regions of Ecuador, through the integration of traditional knowledge and scientific approaches. *J. Ethnobiol. Ethnomed.* **2024**, *20*, 60. [CrossRef]
19. Gutiérrez-Salazar, P.; Ramsay, P.M. Physiognomic responses of páramo tussock grass to time since fire in northern Ecuador. *Rev. Peru. Biol.* **2020**, *27*, 205–214. [CrossRef]
20. Zomer, M.A.; Ramsay, P.M. Post-fire changes in plant growth form composition and diversity in Andean páramo grassland. *Appl. Veg. Sci.* **2021**, *24*, e12554. [CrossRef]
21. Jones, M.W.; Abatzoglou, J.T.; Veraverbeke, S.; Andela, N.; Lasslop, G.; Forkel, M.; Smith, A.J.; Burton, C.; Betts, R.A.; van der Werf, G.R.; et al. Global and Regional Trends and Drivers of Fire Under Climate Change. *Rev. Geophys.* **2022**, *60*, e2020RG000726. [CrossRef]
22. Haas, O.; Keeping, T.; Gomez-Dans, J.; Prentice, I.C.; Harrison, S.P. The global drivers of wildfire. *Front. Environ. Sci.* **2024**, *12*, 1438262. [CrossRef]
23. Ochoa, C.; Bar-Massada, A.; Chuvieco, E. A European-scale analysis reveals the complex roles of anthropogenic and climatic factors in driving the initiation of large wildfires. *Sci. Total Environ.* **2024**, *917*, 170443. [CrossRef] [PubMed]
24. Calviño-Cancela, M.; Chas-Amil, M.L.; García-Martínez, E.D.; Touza, J. Interacting effects of topography, vegetation, human activities and wildland-urban interfaces on wildfire ignition risk. *For. Ecol. Manag.* **2017**, *397*, 10–17. [CrossRef]
25. Román-Cuesta, R.M.; Carmona-Moreno, C.; Lizcano, G.; New, M.; Silman, M.; Knoke, T.; Malhi, Y.; Oliveras, I.; Asbjornsen, H.; Vuille, M. Synchronous fire activity in the tropical high Andes: An indication of regional climate forcing. *Glob. Change Biol.* **2014**, *20*, 1929–1942. [CrossRef]

26. Zapata-Ríos, X.; Lopez-Fabara, C.; Navarrete, A.; Torres-Paguay, S.; Flores, M. Spatiotemporal patterns of burned areas, fire drivers, and fire probability across the equatorial Andes. *J. Mt. Sci.* **2021**, *18*, 952–972. [CrossRef]
27. Díaz, S.C.; Quezada, L.C.; Álvarez, L.J.; Loján-Córdova, J.; Carrión-Paladines, V. Indigenous use of fire in the paramo ecosystem of southern Ecuador: A case study using remote sensing methods and ancestral knowledge of the Kichwa Saraguro people. *Fire Ecol.* **2023**, *19*, 1–18. [CrossRef]
28. Zomer, M.A. Fire Ecology of Northern Andean Grasslands: Estimating Recent fire History and Its Impact on Páramo Plants. Master's Thesis, University of Plymouth, Plymouth, UK, 2016.
29. Oliveras, I.; Anderson, L.O.; Malhi, Y. Application of remote sensing to understanding fire regimes and biomass burning emissions of the tropical Andes. *Glob. Biogeochem. Cycles* **2014**, *28*, 480–496. [CrossRef]
30. Zomer, M.A.; Ramsay, P.M. The impact of fire intensity on plant growth forms in high-altitude Andean grassland. *bioRxiv* **2020**, bioRxiv:2020.04.25.061051. [CrossRef]
31. Vargas-Ríos, O. *Bases Ecológicas y Sociales para la Restauración de los Páramos*; Technical Report; Universidad Nacional de Colombia: Bogota, Colombia, 2021.
32. Zomer, M.A.; Ramsay, P.M. *Espeletia* giant rosette plants are reliable biological indicators of time since fire in andean grasslands. *Plant Ecol.* **2018**, *219*, 79–88. [CrossRef]
33. Luteyn, J.L. Páramos: A checklist of Plant Diversity, Geographical Distribution and Botanical Literature. 1999. Available online: https://lib.icimod.org/records/qyzwy-xmc04/files/235.pdf (accessed on 16 December 2025).
34. Balslev, H.; Luteyn, J.L. *Paramo: An Andean Ecosystem Under Human Influence*; Academic Press: New York, NY, USA, 1992.
35. Curatola Fernández, G.F.; Obermeier, W.A.; Gerique, A.; López Sandoval, M.F.; Lehnert, L.W.; Thies, B.; Bendix, J. Land cover change in the Andes of southern Ecuador-Patterns and drivers. *Remote Sens.* **2015**, *7*, 2509–2542. [CrossRef]
36. Olson, D.M.; Dinerstein, E.; Wikramanayake, E.D.; Burgess, N.D.; Powell, G.V.; Underwood, E.C.; D'Amico, J.A.; Itoua, I.; Strand, H.E.; Morrison, J.C.; et al. Terrestrial ecoregions of the world: A new map of life on Earth: A new global map of terrestrial ecoregions provides an innovative tool for conserving biodiversity. *BioScience* **2001**, *51*, 933–938 [CrossRef]
37. Peyre, G.; Osorio, D.; François, R.; Anthelme, F. Mapping the páramo land-cover in the Northern Andes. *Int. J. Remote Sens.* **2021**, *42*, 7777–7797. [CrossRef]
38. Burbano-Girón, J.; Molina Berbeo, M.A.; Gutiérrez Montoya, C.; Ochoa-Quintero, J.M. *Estado de Conservación de los Páramos en Colombia*; Biodiversidad 2020; Estado y tendencias de la biodiversidad continental de Colombia; Instituto de Investigación de Recursos Biológicos Alexander von Humboldt: Bogotá, Colombia, 2020.
39. Parques Nacionales Naturales de Colombia (PNN). Mapa de áreas Protegidas de Colombia (RUNAP). Shapefile y Metadatos. 2023. Available online: https://storage.googleapis.com/pnn_geodatabase/runap/latest.zip (accessed on 16 December 2025).
40. Instituto de Hidrología Meteorología y Estudios Ambientales (IDEAM); Ministerio de Ambiente y Desarrollo Sostenible (MADS). *Actualización de Cifras de Monitoreo de la Superficie de Bosque—Año 2024; Resumen de Resultados de Monitoreo*; Technical Report; Instituto de Hidrología Meteorología y Estudios Ambientales (IDEAM); Ministerio de Ambiente y Desarrollo Sostenible (MADS): Bogotá, Colombia, 2025.
41. Instituto Geográfico Agustín Codazzi (IGAC). *Cartografía Vectorial a Escala 1:100,000 con Cobertura Total de la República de Colombia*; Instituto Geográfico Agustín Codazzi (IGAC): Bogotá, Colombia, 2022.
42. Centro Nacional de Memoria Histórica (CNMH). *Geoportal de Datos Abiertos: Casos Acciones bélicas*; Centro Nacional de Memoria Histórica (CNMH): Bogotá, Colombia, 2022.
43. Instituto de Hidrología Meteorología y Estudios Ambientales (IDEAM). *Cobertura de la Tierra. Metodología CORINE Land Cover Adaptada para Colombia. Período 2018. República de Colombia. Escala 1:100,000*; Instituto de Hidrología Meteorología y Estudios Ambientales (IDEAM): Bogotá, Colombia, 2021.
44. Abatzoglou, J.T.; Dobrowski, S.Z.; Parks, S.A.; Hegewisch, K.C. TerraClimate, a high-resolution global dataset of monthly climate and climatic water balance from 1958–2015. *Sci. Data* **2018**, *5*, 170191. [CrossRef] [PubMed]
45. Instituto Geográfico Agustín Codazzi (IGAC). *Modelo Digital de Elevación*; SRTM 30 Metros; Instituto Geográfico Agustín Codazzi (IGAC): Bogotá, Colombia, 2011.
46. Correa Ayram, C.; Etter, A.; Díaz-Timoté, J.; Buriticá, S.; Ramírez, W.; Corzo, G. Spatiotemporal evaluation of the human footprint in Colombia: Four decades of anthropic impact in highly biodiverse ecosystems. *Ecol. Indic.* **2020**, *117*, 106630. [CrossRef]
47. Kutner, M.H.; Nachtsheim, C.J.; Neter, J.; Li, W. *Applied Linear Statistical Models*, 5th ed.; McGraw-Hill: New York, NY, USA, 2005. Available online: https://users.stat.ufl.edu/~winner/sta4211/ALSM_5Ed_Kutner.pdf (accessed on 16 December 2025).
48. Collins, L.; McCarthy, G.; Mellor, A.; Newell, G.; Smith, L. Training data requirements for fire severity mapping using Landsat imagery and random forest. *Remote Sens. Environ.* **2020**, *245*, 111839. [CrossRef]
49. Ma, W.; Feng, Z.; Cheng, Z.; Chen, S.; Wang, F. Identifying Forest Fire Driving Factors and Related Impacts in China Using Random Forest Algorithm. *Forests* **2020**, *11*, 507. [CrossRef]
50. Oliveira, S.; Oehler, F.; San-Miguel-Ayanz, J.; Camia, A.; Pereira, J.M. Modeling spatial patterns of fire occurrence in Mediterranean Europe using Multiple Regression and Random Forest. *For. Ecol. Manag.* **2012**, *275*, 117–129. [CrossRef]

51. Breiman, L. Random forests. *Mach. Learn.* **2001**, *45*, 5–32. [CrossRef]
52. Friedman, J.H. Greedy Function Approximation: A Gradient Boosting Machine on JSTOR. *Ann. Stat.* **2001**, *2001*, 1189–1232. [CrossRef]
53. Hijmans, R. terra: Spatial Data Analysis. R Package Version 1.8-73. 2025. Available online: https://rspatial.org/ (accessed on 16 December 2025).
54. Taiyun, W.; Viliam, S. R Package 'Corrplot': Visualization of a Correlation Matrix (Version 0.95). 2024. Available online: https://github.com/taiyun/corrplot (accessed on 16 December 2025).
55. Zhang, X.; Lu, X.; Wang, X. Spatial-Temporal NDVI Variation of Different Alpine Grassland Classes and Groups in Northern Tibet from 2000 to 2013. *Mt. Res. Dev.* **2015**, *35*, 254–263. [CrossRef]
56. Chuvieco, E.; Cocero, D.; Riaño, D.; Martínez-Vega, J.; de la Riva, J.; Pérez, F. Combining NDVI and surface temperature for the estimation of live fuel moisture content in forest fire danger rating. *Remote Sens. Environ.* **2004**, *92*, 322–331. [CrossRef]
57. Podwojewski, P.; Poulenard, J. La Degradación de los Suelos de los Páramos Risque Hydrométéorologique à Quito View Project PALAS: PAleoclimate from LAke Sediments on Kerguelen Archipelago View Project. 2000. Available online: https://www.researchgate.net/publication/285589451 (accessed on 16 December 2025).
58. Anderson, E.P.; Marengo, J.; Villalba, R.; Halloy, S.; Young, B.; Cordero, D.; Gast, F.; Jaimes, E.; Ruiz, D. Consequences of climate change for ecosystems and ecosystem services in the tropical Andes. In *Climate Change and Biodiversity in the Tropical Andes*; Herzog, S.K., Martínez, R., Jørgensen, P.M., Tiessen, H., Eds.; Inter-American Institute for Global Change Research (IAI): Ciudad del Saber, Edificio; Scientific Committee on Problems of the Environment (SCOPE): Paris, France, 2011; pp. 1–18.
59. Vargas, O. Sucesión-Regeneración del páRamo Después de Quemas. Available online: https://repositorio.unal.edu.co/handle/unal/50412 (accessed on 16 December 2025).
60. Convention on Biological Diversity (CBD). *Colombia: Country Dossier 2021—National Biodiversity Strategy and Action Plan/Protected Areas Management Effectiveness*; Technical Report; Convention on Biological Diversity (CBD): Rio de Janeiro, Brazil, 2021. Available online: https://www.cbd.int/pa/doc/dossiers/colombia-abt11-country-dossier2021.pdf (accessed on 16 December 2025).